

Stretchable Shape-sensing Ribbons

Stephanie J. Woodman, Anjali Agrawala, and Rebecca Kramer-Bottiglio

Mechanical Engineering and Materials Science

Yale University

New Haven, CT, USA

stephanie.woodman@yale.edu

Abstract—Future robots will boast mutable morphology, properties, and behavioral control policies to adapt to changing tasks and environments. Soft robots offer an appealing platform for adaptive shape change, as the constituent soft components may stretch and reform into new target shapes. Typical soft robot proprioception and control are achieved by embedding stretch sensors into a robot’s body at locations of anticipated strain during task performance. By mapping the neutral length of those sensors to the neutral (unactuated) shape of the robot, shape changes are detected when the sensors deviate from those positions. However, this approach relies on a fixed neutral shape and corresponding mechanics model, which is not the case for shape-changing robots. To introduce a mechanics-model-free approach to shape estimation for shape-changing robots, we report a sensory ribbon that fuses stretch and orientation data to reconstruct the 3D shape of the ribbon in free space and apply it to the surface of arbitrary host objects.

Index Terms—shape sensing, soft robotics, shape-change

I. INTRODUCTION

It is generally accepted that there are optimal forms for any desired function [1], which has led to the pursuit of shape-changing robots that can adapt their morphology and behavioral control policy towards changing tasks and environments [2]. Such adaptive shape-change is uniquely possible with soft robot platforms, due to the inherent stretchability and morphability of soft materials and components [3]–[7].

Shape-changing robots require closed-loop shape control. However, current soft robot proprioception, state estimation, and control approaches are not amenable to changes in neutral body shape. The typical approach is to 1) embed stretchable sensors—either resistive or capacitive [8]–[10]—into the body or surface of a soft robot, 2) note the sensor readings when the robot is unactuated and in its neutral shape, and 3) infer actuation and motion from sensor readings that deviate from those corresponding to the neutral shape. Coupled with mechanics and kinematics models of the robot’s shape, this simple approach is effective when the neutral shape of the robot is unchanging. However, for robots with mutable shapes, a new model-free approach is needed.

A model-free approach is possible: a surface shape can be reconstructed with measurements of orientation at multiple points along the surface and the distance between each of the points [11], [12]. This approach has previously been

This material is based upon work supported by the National Science Foundation under IIS-1954591. S.J.W. was supported by a NASA NSTGRO Fellowship (80NSSC22K1188). A.A. was supported by an NSF Graduate Research Fellowship, DGE-2139841.

used to construct inextensible shape-sensing arrays [13]–[15]. However, for inextensible arrays, information is lost when the subject stretches or deforms (*i.e.*, if the underlying body stretches—thereby changing the distance between the sensors—the approach fails). Mathematically, the Nyquist-Shannon sampling theorem states that for any single curve, at least two tangents pointing along the curve are required to determine the curvature κ , but this yields no information about scale [16]. We, therefore, surmise that introducing stretchable strain sensors between orientation sensors should yield extensible shape-sensing arrays that can measure both the surface shape and scale of an underlying body.

In previous work, we attempted to realize robust shape estimation via a platform fusing orientation sensors and stretchable circuits. Our work used embedded liquid-metal capacitive strain sensors that dynamically measure the distance between orientation sensors [17]. However, interfacing the silicon integrated circuits with soft substrates and conductors proved challenging—a problem that has been independently addressed in the literature [18]—and we were previously unable to measure curvatures and stretch simultaneously.

Herein, we present a sensing platform that positions stretchable, textile-based capacitive strain sensors that can be easily fabricated from readily accessible materials [19] between off-the-shelf 9-axis orientation sensor breakout boards (BNO055, Adafruit, Inc.) (Fig. 1a-c). Using this platform, for the first time, we illustrate the benefits of stretch in surface-based shape sensing and demonstrate the platform’s potential utility in closed-loop shape control for emerging shape-changing systems. We validate the platform’s accuracy on shapes with increasing sinusoidal frequency, as well as increasing feature amplitudes and correspondingly increased perimeter lengths. Our results show that the incorporation of the stretch sensors between the orientation sensors allows the system to fully reconstruct the target shapes and length scales.

II. FABRICATION AND EXPERIMENTAL METHODS

Our sensing system is a ribbon consisting of six stretch sensors and six orientation sensors (Fig. 1c-d). The ribbon of stretchable sensors was fabricated first. As illustrated in Fig. 1e (and further detailed in [19]), each sensor is multi-layered: an outer electrode made of stretchable, conductive fabric wraps around two layers of a stretchable, non-conductive fabric dielectric and an inner electrode. All layers are adhered with a stretchable textile adhesive. This layering architecture forms

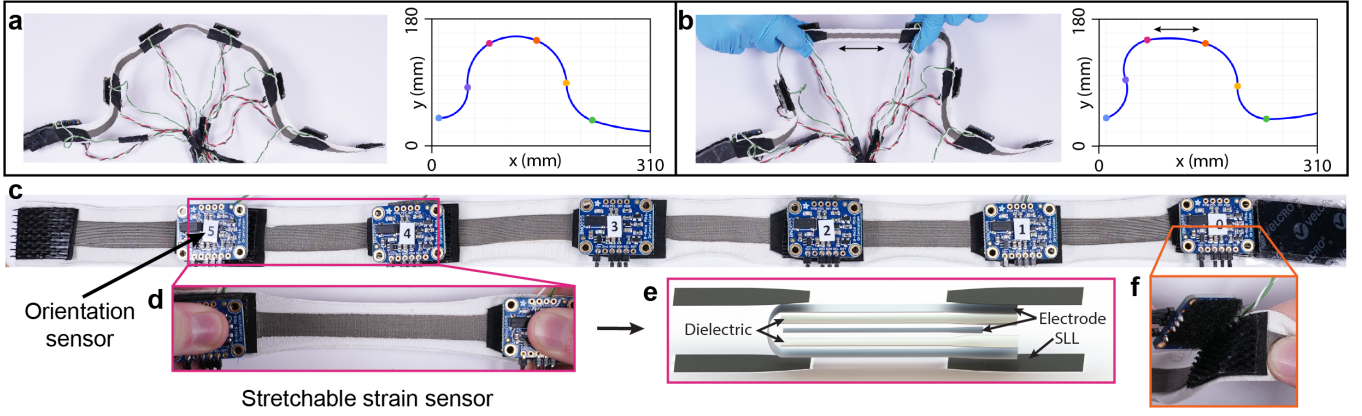


Fig. 1. **Overview and fabrication.** **a**, Un-stretched and **b**, stretched sensor ribbon and measured shape. **c**, Sensor ribbon laid flat. **d**, Strain sensor stretched. **e**, Exploded view of strain sensor; SLL denotes strain-limiting layer. **f**, Velcro attachment of orientation sensor to sensing ribbon.

a parallel plate capacitor such that when the sensor undergoes strain, the capacitance increases. The five-layer design shields the sensor from sensitivity to twisting or external pressures.

To derive the relation between capacitance change and displacement (sensor length), five sensor samples were strained on a mechanical testing device (Instron 3345) while measuring capacitance, and a quadratic equation was fit to the averaged data (Fig. 2). In the full ribbon system, one dielectric fabric layer is common across each of the six sensors. Strain-limiting layers of inextensible woven fabric were placed at the ends of each sensor to support the orientation sensor breakout boards, which were secured by Velcro (Fig. 1f). The ends of the ribbon also had Velcro to close the ribbon during testing.

To collect data and estimate shape, each strain sensor was interfaced with a capacitive sensor processing board (MPR121, Adafruit, Inc.; rise time = 1 μ s, charge current = 39 μ A), and each orientation sensor was interfaced with a multiplexer (TCA9548A, Adafruit, Inc.). The processing board and the multiplexer were connected to a microprocessor breakout board (Arduino Nano, Arduino). The shape estimations were obtained using spherical interpolation (commonly referred to as ‘‘Slerp,’’ [20]) between the six orientations, with the strain sensor providing the distance between each orientation.

To evaluate the utility and accuracy of the shape-sensing ribbon, we generated twelve shapes with various radial frequencies and amplitudes/perimeters, mimicking the effects of expansion of soft actuators on a robot body. We generated these shapes using Equation (1), where $r(\Theta)$ gives the polar coordinates of the output shape, r_{mean} is the mean radius of a circle, A is the amplitude of surface features, ω is the radial frequency of surface features, ϕ is the phase (always zero for our shapes), and Θ is the angle from the polar axis.

$$r(\Theta) = r_{mean}(1 + A \sin(\omega\Theta + \phi)) \quad (1)$$

In Fig. 3, from left to right, radial frequency increases from 0 to 2, 3, and 4; From top to bottom, the amplitude of the radial features and shape perimeter length are increased to set the ribbon’s strain to 0%, 20%, and 40%, respectively. In more

detail, the dimensions of the two-dimensional shapes are as follows. **Fig. 3a-d**: perimeter of 480 mm (the unstrained length of the ribbon, thus the ribbon is at 0% strain applied around the perimeter) and amplitude of 0.2; **Fig. 3e-h**: perimeter of 580 mm (20% strain) and amplitude of 0.3; **Fig. 3i-l**: perimeter of 680 mm (40% strain) and amplitude of 0.4. The shapes were laser cut out of acrylic (ULS VLS 2.30DT).

The sensing ribbon was wrapped around each shape five times. The shape measurement was calculated during post-processing, along with finding the mean absolute error (MAE) between the experimentally measured shape and the ground truth shape, provided by the CAD model. The smallest Euclidean distance was found between each data point in the measured shape and points along the ground truth shape. These distances were averaged to find the MAE of each trial. The MAE values were then averaged across the five samples, yielding the reported cumulative MAE value in Fig. 3.

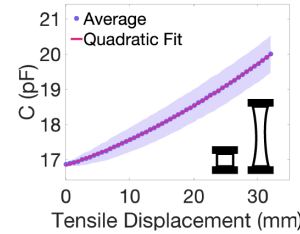


Fig. 2. **Sensor characterization.** Capacitance vs. displacement from five sensor samples, and the quadratic fit ($R^2 = 0.999$) used to approximate stretch in the sensing ribbon. Cloud represents one standard deviation.

III. RESULTS

The sensing ribbon is able to capture sinusoidal curvatures with radial frequencies 0, 2, and 3 with relatively low MAEs, even as the amplitude and perimeter increase. We note a sharp increase in the MAE for a radial frequency of 4, which is expected, as there are no longer enough orientation sensors to capture the additional curvatures.

Average MAE increases across each radial frequency as strain increases. This loss of accuracy at higher strains could be due to increased sensor-to-sensor variation at displacements greater than 10 mm, as seen in Fig. 2. Despite the increase in MAE, the system is still able to reasonably capture the

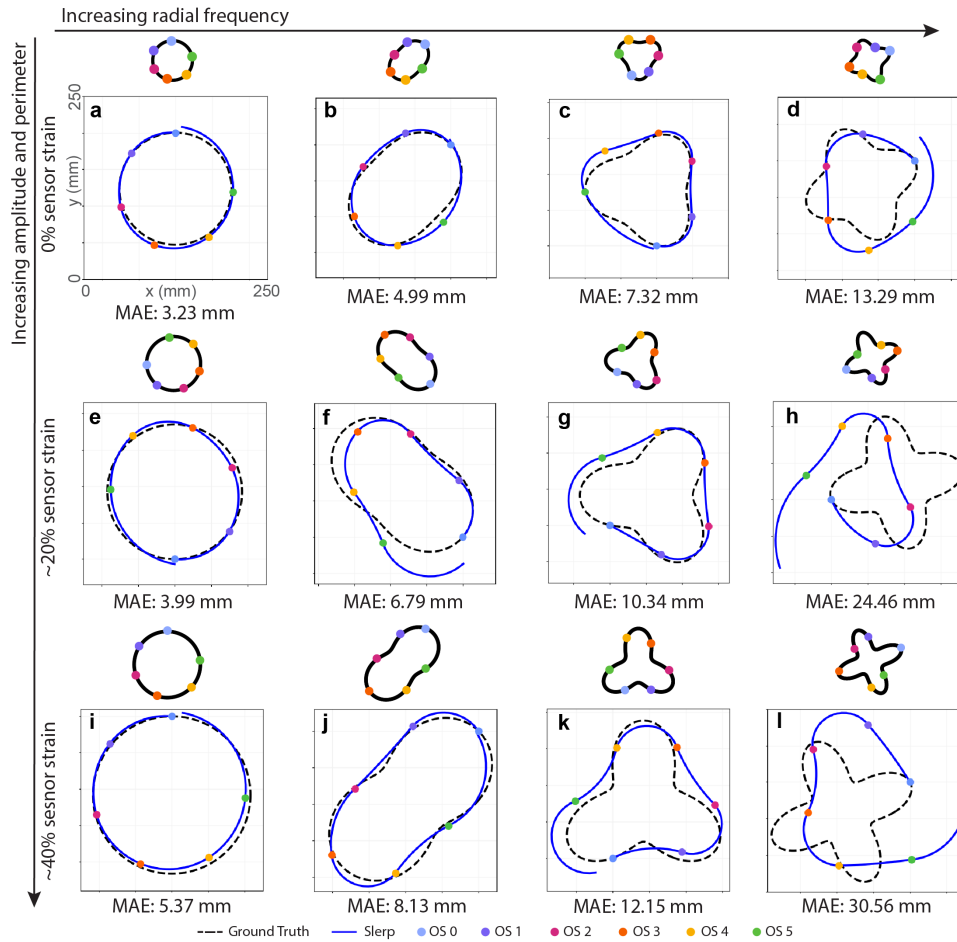


Fig. 3. **Average MAE with increasing strain/amplitude, and radial frequency.** Representative samples of the shape measurements (blue curves) compared to the ground truth shapes (dotted lines), for each shape tested. Locations of the orientation sensors (OS) are denoted on the estimated shape, and their true location is also shown in the schematic of the ground-truth shape above each test. MAE values were averaged over five trials, and the axes and scale in (a) apply to all subplots.

curvature and size of shapes with ≤ 3 radial sinusoids and with amplitudes and/or perimeters that correspond to $\leq 40\%$ ribbon strain. With an inextensible system, only the shapes in Fig. 3a-c (0% strain) would have been accurately captured. Using stretchable sensors, the shapes in Fig. 3e-g,i-k are measurable.

IV. DISCUSSION

The results herein indicate that, as long as the number of orientation sensors is at least double that of the target object's radial frequency, the stretchable sensing ribbon can capture changes in both shape and scale of shape-changing hosts.

Because the sensor ribbon is designed to be general-purpose, we did not tailor sensor placement to best capture each tested shape. Consequently, we noticed difficulties capturing both shallow curvatures, as in Figs. 3c, f, & j, and very sharp curvatures, as in Fig. 3k. We suspect that capturing shallow curvatures with the sensor ribbon was difficult because compliance in the Velcro attachment of the orientation sensors led to the orientation sensors not lying perfectly tangent to the shape. Capturing sharp curvatures was difficult because the orientation sensors were not placed intentionally close to sharp

curves, and the measurement method smoothly interpolates between the orientation measurements. With a higher sensor density, sharper curvatures could be captured, but at the cost of an increasingly complex system.

The inextensible attachment mechanism that linked the ends of the sensing ribbon led to the slightly asymmetric placement of orientation sensors, which may have affected the accuracy of reconstructing concave curvatures, as in Fig. 3c, between orientation sensor 0 and orientation sensor 5. Without the asymmetry, this concave curvature would have been capturable, as validated by the concave curvatures in Fig. 3g & k, where the asymmetry is minimized with higher strains.

This work serves as a step towards shape estimation for topologically complex systems and will enable closed-loop shape control of next-generation shape-changing robots. In future work, we will improve upon the sensor ribbon design by augmenting the hardware and shape reconstruction algorithms to work for three-dimensional (3D) shape estimation. Future experiments will include expanded sensor arrays and tests on dynamically shape-shifting 3D platforms.

REFERENCES

- [1] R. Pfeifer and J. Bongard, *How the body shapes the way we think: a new view of intelligence*. MIT press, 2006.
- [2] D. Shah, B. Yang, S. Kriegman, M. Levin, J. Bongard, and R. Kramer-Bottiglio, "Shape Changing Robots: Bioinspiration, Simulation, and Physical Realization," *Advanced Materials*, vol. 33, p. 2002882, may 2021.
- [3] E. Steltz, A. Mozeika, N. Rodenberg, E. Brown, and H. M. Jaeger, "JSEL: Jamming skin enabled locomotion," *2009 IEEE/RSJ International Conference on Intelligent Robots and Systems, IROS 2009*, pp. 5672–5677, dec 2009.
- [4] D. S. Shah, J. P. Powers, L. G. Tilton, S. Kriegman, J. Bongard, and R. Kramer-Bottiglio, "A soft robot that adapts to environments through shape change," *Nature Machine Intelligence 2020 3:1*, vol. 3, pp. 51–59, nov 2020.
- [5] R. Baines, S. Freeman, F. Fish, and R. Kramer-Bottiglio, "Variable stiffness morphing limb for amphibious legged robots inspired by che- lonian environmental adaptations," *Bioinspiration Biomimetics*, vol. 15, p. 025002, feb 2020.
- [6] H. T. Lin, G. G. Leisk, and B. Trimmer, "GoQBot: a caterpillar- inspired soft-bodied rolling robot," *Bioinspiration Biomimetics*, vol. 6, p. 026007, apr 2011.
- [7] R. Baines, S. K. Patiballa, J. Booth, L. Ramirez, T. Sipple, A. Garcia, F. Fish, and R. Kramer-Bottiglio, "Multi-environment robotic transitions through adaptive morphogenesis," *Nature*, vol. 610, no. 7931, pp. 283–289, 2022.
- [8] S. Seyedin, P. Zhang, M. Naebe, S. Qin, J. Chen, X. Wang, and J. M. Razal, "Textile strain sensors: a review of the fabrication technologies, performance evaluation and applications," *Materials Horizons*, vol. 6, no. 2, pp. 219–249, 2019.
- [9] B. Shih, D. Shah, J. Li, T. G. Thuruthel, Y. L. Park, F. Iida, Z. Bao, R. Kramer-Bottiglio, and M. T. Tolley, "Electronic skins and machine learning for intelligent soft robots," *Science Robotics*, vol. 5, p. 9239, apr 2020.
- [10] H. Souri, H. Banerjee, A. Jusufi, N. Radacsi, A. A. Stokes, I. Park, M. Sitti, and M. Amjadi, "Wearable and stretchable strain sensors: materials, sensing mechanisms, and applications," *Advanced Intelligent Systems*, vol. 2, no. 8, p. 2000039, 2020.
- [11] N. Sprynski, N. Szafran, B. Lacolle, and L. Biard, "Surface recon- struction via geodesic interpolation," *Computer-Aided Design*, vol. 40, pp. 480–492, apr 2008.
- [12] T. Stanko, S. Hahmann, G. P. Bonneau, and N. Saguin-Sprynski, "Shape from sensors: Curve networks on surfaces from 3D orientations," *Computers Graphics*, vol. 66, pp. 74–84, aug 2017.
- [13] A. Hermanis, R. Cacurs, and M. Greitans, "Acceleration and Magnetic Sensor Network for Shape Sensing," *IEEE Sensors Journal*, vol. 16, pp. 1271–1280, mar 2016.
- [14] T. Hoshi and H. Shinoda, "3D shape measuring sheet utilizing grav- itational and geomagnetic fields," *Proceedings of the SICE Annual Conference*, pp. 915–920, 2008.
- [15] P. Mittendorfer, E. Dean, and G. Cheng, "3D spatial self-organization of a modular artificial skin," *IEEE International Conference on Intelligent Robots and Systems*, pp. 3969–3974, oct 2014.
- [16] C. E. Shannon, "Communication in the Presence of Noise," *Proceedings of the IRE*, vol. 37, no. 1, pp. 10–21, 1949.
- [17] D. S. Shah, S. J. Woodman, L. Sanchez-Botero, S. Liu, and R. Kramer- Bottiglio, "Stretchable Shape-sensing Sheets," *Under review at Ad- vanced Intelligent Systems*, 2023.
- [18] D. F. Fernandes, C. Majidi, and M. Tavakoli, "Digitally printed stretch- able electronics: a review," *Journal of Materials Chemistry C*, vol. 7, pp. 14035–14068, nov 2019.
- [19] L. Sanchez-Botero, A. Agrawala, and R. Kramer-Bottiglio, "Stretchable, breathable, and washable fabric sensor for human motion monitoring.," *Advanced Materials Technologies (Accepted)*.
- [20] K. Shoemake, "Animating rotation with quaternion curves," in *Proceed- ings of the 12th annual conference on Computer graphics and interactive technologies*, pp. 245–254, ACM Digital Library, 1985.